Substrate Specificity in Short-Chain Phospholipid Analogs at the Active Site of Human Synovial Phospholipase A_2

Thomas N. Wheeler,*,† Steven G. Blanchard,*,‡ Robert C. Andrews,† Frank Fang,† Yolanda Gray-Nunez,† Cole O. Harris,‡ Millard H. Lambert,‡ Mukund M. Mehrotra,† Derek J. Parks,‡ John A. Ray,† and Terrence L. Smalley, Jr.†

Divisions of Medicinal Chemistry and Molecular Science, Glaxo Research Institute, 5 Moore Drive, Research Triangle Park, North Carolina 27709

Received April 6, 1994[⊗]

The substrate specificity at the active site of recombinant human synovial fluid phospholipase A_2 (hs-PLA_2) was investigated by the preparation of a series of short-chain phospholipid analogs and measurement of their enzymatic hydrolysis at concentrations well below the critical micelle concentration. Substrates used in the study included 1,2-dihexanoylglycerophospholipids, 1,2-bis(alkanoylthio)glycerophospholipids, and 1-*O*-alkyl-2-(alkanoylthio)phospholipids. Turnover was observed for only a few of the 1,2-dihexanoylglycerophospholipids, and the rate of hydrolysis was very low, near the limit of detection of the assay. In contrast, selected 2-(alkanoylthio)-glycerophospholipids were hydrolyzed by hs-PLA_2 at much higher rates at concentrations well below their critical micelle concentration (cmc). Thus, the 1,2-bis(hexanoylthio)glycerophosphatidylmethanol exhibits a k_{cat}/K_M = 1800 L mol^{-1} s^{-1}. Over the calculated log *P* (cLogP) range of 3-9, cLogP and $\log(k_{cat}/K_M)$ were linearly related for compounds with straight-chain *sn*-1 and *sn*-2 substituents. At comparable cLogP's, the *sn*-1 ethers and thioesters were hydrolyzed at comparable rates. A negative charge in the phosphate head group was required for enzyme activity. Unsaturation, aromaticity, and branching in the *sn*-2 substituent reduce turnover dramatically. The same structural modifications in the *sn*-1 substituent have less effect on turnover. Certain of these substrates, e.g., 1,2-bis(hexanoylthio)glycerophosphatidylmethanol, may be useful in assaying for active site inhibitors of PLA_2. The structure-activity relationships established here for substrates should serve as a reference for the structure-activity relationships of substrate-based inhibitors.

Introduction

Phospholipase A_2's are enzymes which hydrolyze membrane glycerophospholipids at the *sn*-2 position to liberate free fatty acids, including arachidonic acid, and lysophospholipids, both of which are precursors to several known proinflammatory mediators (prostaglandins, leukotrienes, and platelet activating factor).[1] Human synovial phospholipase A_2 (hs-PLA_2) is a low molecular weight (14 kDa), Ca^{2+}-dependent, extracellular enzyme secreted in response to inflammatory stimuli, e.g., by synoviocytes when stimulated by IL-1. This enzyme is elevated in the synovial fluid of arthritic joints, and the PLA_2 levels correlate with the severity of the disease.[2] Synovial PLA_2 is found in high levels in the serum of endotoxic shock patients,[3] and the enzyme has been reported to produce a local inflammatory response when injected *in vivo*.[4] Because of their involvement with these and other inflammatory processes, inhibitors of hs-PLA_2 have been regarded as potential therapeutically useful targets, and assay methods for the evaluation of hs-PLA_2 inhibitors have been the subject of considerable investigation.

Endogenous phospholipid is present almost totally in aggregated form, and PLA_2's, including hs-PLA_2, have evolved to hydrolyze aggregated substrate. Thus, phospholipase A_2's exhibit kinetics which reflect both substrate hydrolysis and enzyme partitioning between the aqueous environment and the lipid-aqueous interface. For aggregated substrates, the apparent substrate specificity of the enzyme is a function of both formation of the substrate-enzyme complex and enzyme binding to the membrane surface. In order to characterize the substrate specificity due to binding at the active site, it is necessary to remove (or hold constant) the contribution of enzyme partitioning to the observed kinetics.

One approach to this problem that has been successfully applied to the hs-PLA_2 is analysis of hydrolysis in the "scooting" mode.[5a,b] The scooting assay monitors the kinetics of interfacial hydrolysis of phospholipid substrates by hs-PLA_2 under conditions where the enzyme does not leave the strongly anionic phospholipid vesicle interface.

We have employed an alternative *yet precedented*[5c,d] approach in which short-chain phospholipid substrate analogs were synthesized and their hydrolysis by PLA_2 was studied at varying substrate concentrations. Measurement of their hydrolytic cleavage by hs-PLA_2 at concentrations well below the corresponding critical micelle concentrations (cmc) provided information on the structural preferences of PLA_2 for substrates *in the absence of a membrane surface*. Under these conditions, therefore, the observed kinetic parameters are a reflection solely of substrate interaction with the active site of the enzyme. The resulting information should prove useful in the design of active site directed inhibitors of hs-PLA_2.

During the course of this work, a variety of novel substrates were "docked" into a model hs-PLA_2 in an effort to explain the experimental structure-activity relationship. The model structure for hs-PLA_2 was

* Authors to whom inquiries should be directed.
† Division of Medicinal Chemistry.
‡ Division of Molecular Science.
⊗ Abstract published in *Advance ACS Abstracts*, October 15, 1994.

0022-2623/94/1837-4118$04.50/0

constructed from X-ray structures of bovine pancreatic[6] and snake venom[7] PLA_2. The model structure proved to be similar to subsequently published structures of hs-PLA_2.[8,9] An X-ray structure of an amide substrate-based inhibitor, (*R*)-2-(dodecanoylamino)-1-hexanol phosphoglycol, bound to a mutant pancreatic PLA_2,[10] was then used to construct models for ester and thioester substrates bound to hs-PLA_2. In the calculated structures, the *sn*-3 phosphate head group binds to the calcium and to the side-chain amino group of Lys-69. The *sn*-2 ester or thioester group binds at the bottom of the active site cavity, between the calcium ion and His-48. The *sn*-2 tail undergoes a sharp change in direction at the first bond beyond the ester or thioester group and is then directed through a narrow lipophilic channel to the surface of the enzyme. The *sn*-1 tail is directed through a somewhat wider lipophilic channel, parallel and adjacent to the *sn*-2 tail. The binding mode remains similar to that of the amide inhibitor and is also generally similar to the subsequently determined binding modes of a phosphonate inhibitor bound to cobra-venom PLA_2[11] and hs-PLA_2.[9]

Biological Results

The initial strategy for the investigation of substrate specificity involved the synthesis of a series of 1,2-dihexanoylglycerophospholipids (**6a–g**) with variation in the phosphate head group. Hydrolysis was followed by titration of released protons.[12,13] Under the assay conditions described, the detection limit was ~2–5 nmol·min^{-1}·mg^{-1}. For the phosphatidylethanolamine (**6a**) the turnover was confirmed by an independent method in which the amine head group was reacted with excess fluorescamine, and the resulting fluorescent derivatives were quantified by reversed-phase HPLC. This method gave a value of 2.3 nmol·min^{-1}·mg^{-1}, in good agreement with the pH-stat method.

Turnover was observed for only a few of the substrates listed in Table 1, and the experimental values were at, or near, the limits of detection for the assay. In contrast to these results, the thioester analog **12d** (Table 2) gave a value of 80 nmol·min^{-1}·mg^{-1} when assayed by the pH-stat method under identical conditions. On the basis of this result, a series of 1,2-bis(alkanoylthio)glycerophospholipids was prepared and tested.

Table 2 shows that (with the exception of the shortest chain member) a series of 1,2-bis(alkanoylthio)glycerophospholipids are hydrolyzed at a significantly higher rate than the corresponding oxyesters.[14,15]

A plot of the initial rate of hydrolysis vs [S] is linear up to the highest concentration of substrate tested (100 μM) for all of the substrates described in this study. Figure 1 illustrates this for 1,2-bis(hexanoylthio)phosphatidylmethanol, **12d**. The results are consistent with Michaelis–Menten kinetics under conditions where [S] $\ll K_M$ and suggest that hs-PLA_2 hydrolyzes these substrates as the monomeric species under the conditions employed. Under these conditions the slope of such plots is linear and the *apparent* k_{cat}/K_M values were obtained by dividing the experimentally determined slope by the (known) enzyme concentration. Figure 2 shows that a plot of hydrolytic rate of **12d** vs enzyme concentration at constant [S] is linear at concentrations of enzyme up to 10-fold higher than those used for the estimation of the k_{cat}/K_M values of the substrates. This plot is also consistent with Michaelis–Menten kinetics. Deviation from linearity in these plots would suggest more complex behavior, e.g., enzyme-induced microaggregation of substrate.

Table 2 suggests a correlation between the length of the *sn*-1 and *sn*-2 chains and substrate activity. This relationship is illustrated in Figure 3 where chain length is expressed as the number of methylenes, *n*, in the two side chains. Detectable hydrolysis was observed where $n > 1$ (propionyl). Extension of both acyl chains by a single methylene group resulted in both a signifi-

Table 1. Specific Activity of 1,2-Dihexanoylglycerophospholipid Monomeric Substrates for hs-PLA_2

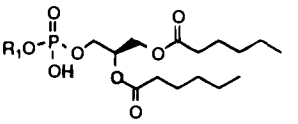

	R_1	Hydrolysis (nmol min^{-1}mg^{-1})	CMC (mM)
6a		5.3 (2.3)[a]	-
6b		<5	-
6c	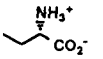	<5	-
6d	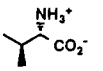	<5	-
6e		<5	-
6f		13	0.5
6g		12	0.8

[a] Determined by the fluorescamine procedure. [b] cmc's determined from plots of the fluorescence intensity of 8-anilino-1-naphthalenesulfonic acid as a function of compound concentration.[16]

Table 2. Specific Activity of 1,2-Bis(alkanoylthio)glycerophospholipids as Monomeric Substrates

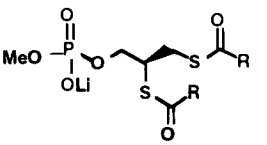

compd	R	k_{cat}/K_M (L mol^{-1} s^{-1})	cmc (mM)	cLogP
12a	CH_3CH_2	<10	≥3	2.31
12b	$CH_3(CH_2)_2$	200	2.3	3.37
12c	$CH_3(CH_2)_3$	870	>9	4.42
12d	$CH_3(CH_2)_4$	1800	≥3	5.48
12e	$CH_3(CH_2)_5$	37700	0.3	6.54
12f	$CH_3(CH_2)_6$	408000	0.03	7.60
12g	$CH_3(CH_2)_7$	541000	<0.03	8.66

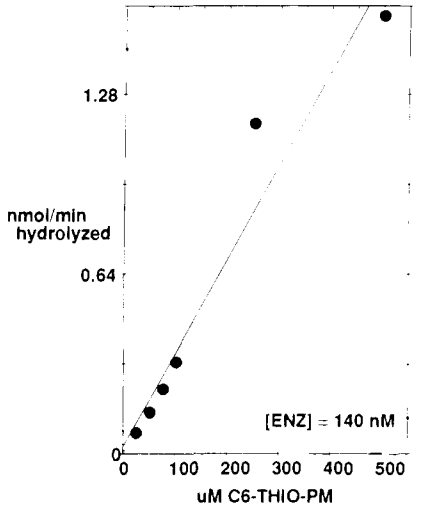

Figure 1. Plot of initial rate of hydrolysis of **12d** vs substrate concentration.

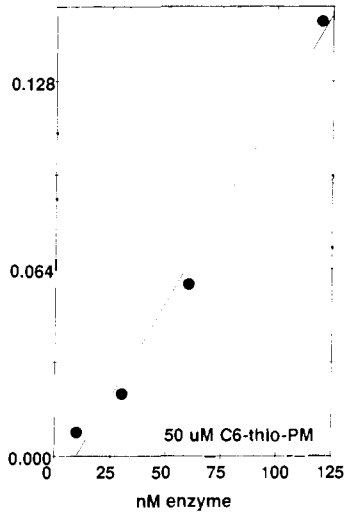

Figure 2. Plot of initial rate of hydrolysis of **12d** vs enzyme concentration.

cant increase in k_{cat}/K_M and a decrease in the critical micelle concentration. The plot is linear up to $n = 6$. Note that the slope of the line appears to be independent of the state of substrate aggregation. Thus, there is no apparent "break" in the slope when n is increased from 5 to 6 even though the cmc measurements suggest that the substrate should be aggregated when $n = 6$ but monomeric for $n = 5$. cmc's were determined in the same buffer lacking DTNB but containing 5 μM 8-1-ANS.[16]

Table 3 indicates that 1-*O*-alkyl-2-(alkanoylthio)-glycerophospholipids are also substrates for hs-PLA_2 and that they show quite similar behavior to the dithioesters.

Figure 4 illustrates that the apparent k_{cat}/K_m of the phospholipid substrate analogs is dependent on lipophilicity. A plot of cLogP vs log (k_{cat}/K_M) gives a straight line with slope = 1.24, intercept = 1.20, and correlation coefficient = 0.963. This linear relationship is not limited to 1,2-bis(alkanoylthio)glycerophospholipids. The data points shown in Figure 4 include compounds with *sn*-1 ether substituents as well as *sn*-1 thioester substituents.

Other structural features in addition to lipophilicity are important to the substrate specificity of these short-

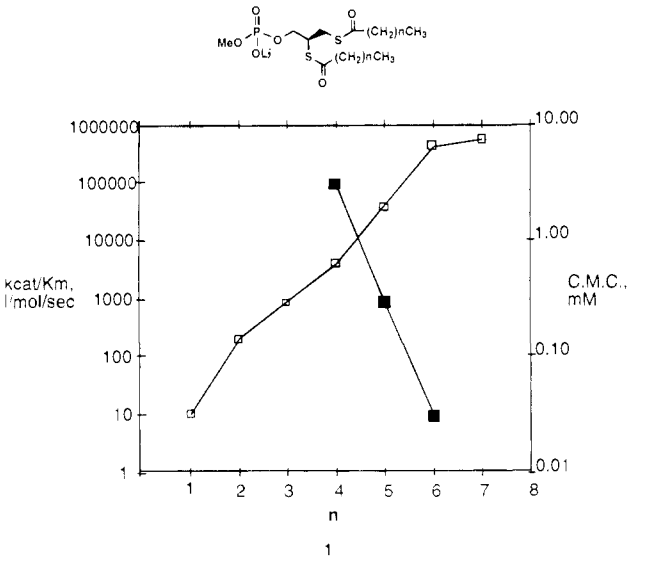

Figure 3. Plot of substrate activity and critical micelle concentration vs length of the *sn*-1 and *sn*-2 chains, expressed as the number n of methylenes. Compound **12a**, which is listed in Table 2 with $k_{cat}/K_M < 10$ L mol^{-1} s^{-1}, is plotted here as the upper limit.

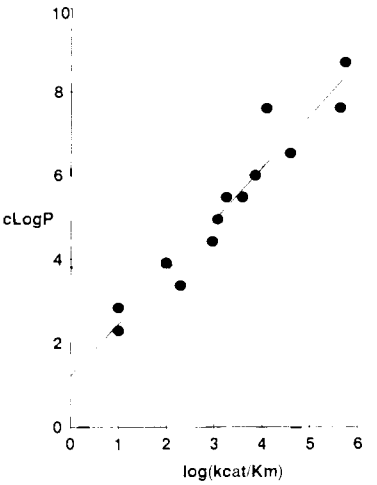

Figure 4. Plot of lipophilicity, expressed as the cLogP,[15] vs substrate activity, expressed as log (k_{cat}/K_M). Compounds **12a**, **22a**, and **22c**, which are listed in Tables 2 and 3 with k_{cat}/K_M <10 or <100 L mol^{-1} s^{-1}, are plotted here as the upper limits.

Table 3. Specific Activity of 1-*O*-Alkyl(alkanoylthio)glycerophospholipids as Monomeric Substrates

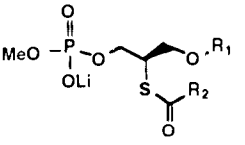

	R_1	R_2	k_{cat}/K_M (L mol^{-1} s^{-1})	cmc (mM)	cLogP
22a	$CH_3(CH_2)_2$	$CH_3(CH_2)_2$	<10	3.0	2.83
22b	$CH_3(CH_2)_2$	$CH_3(CH_2)_6$	1200	1.0	4.95
22c	$CH_3(CH_2)_4$	$CH_3(CH_2)_2$	<100		3.89
22d	$CH_3(CH_2)_4$	$CH_3(CH_2)_6$	7000	1.25	6.01
22e	$CH_3(CH_2)_7$	$CH_3(CH_2)_2$	3700	0.25	5.48
22f	$CH_3(CH_2)_7$	$CH_3(CH_2)_6$	12000	0.13	7.60

chain phospholipids. Table 4 illustrates that a negative charge in the phosphate head is essential for enzyme activity.

Table 3 indicates that the replacement of the *sn*-1 thioester group with an ether substituent does not

Table 4. Importance of a Negative Charge in the Phosphate Head

compd		k_{cat}/K_M (L mol^{-1} s^{-1})	cmc (mM)
12d	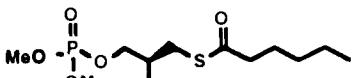	1800	3.0
11d	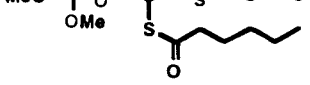	<100	0.04

Table 5. Effect of C_1 Variation on Specific Activity and cmc

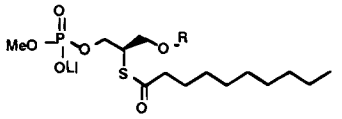

	R	kcat/KM (L mol^{-1}sec^{-1})	CMC (mM)	cLog P
22g	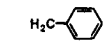	5,000	0.2	6.49
22h	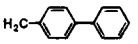	2,500	0.10	8.38
22i	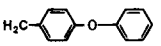	4,600	0.04	8.59
22j	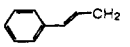	19,000	0.04	7.12
22k	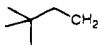	627	0.4	7.34
22l		5,900	0.2	7.05

reduce substrate activity provided the *sn*-1 and *sn*-2 chain lengths are adjusted to maintain comparable lipophilicity. Table 5 demonstrates that aromaticity, unsaturation, and chain branching are tolerated in the *sn*-1 substituent.

The model structure, and the X-ray structures upon which it is based, show a well-defined and relatively narrow lipophilic pocket which accommodates the *sn*-2 substituent of the glyceryl phospholipids. The calculated structures indicated that the *sn*-2 tail must undergo a sharp change in direction at the first rotatable bond beyond the thioester group to avoid collision with Cys-45 and Phe-106 in hs-PLA_2. Docking calculations indicated that compound **22p** (Table 6) could not fit into the binding site properly because of its rigidity. This compound was thus predicted to be inactive and was synthesized to test the hypothesis. Docking calculations indicated that compounds **22m**, **22n**, and **22o** were flexible enough to undergo the expected change of direction. It seemed clear that the *trans* double bond of **22o** should fit into the *sn*-2 channel. However, it was not clear from graphical examination of the calculated structures whether the *sn*-2 channel could accommodate the branching in **22m** and **22n**. These compounds were thus synthesized to test the ability of the enzyme to accommodate additional width in this position. Surprisingly, all four compounds were found to be very poor substrates (Table VI). Comparison of the compounds in Table 6 with those having a similar cLogP in Table

Table 6. Impact of Variation at C_2 on Substrate Activity

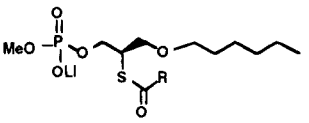

	R	kcat/KM	cLog P
22m	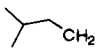	<100	5.35
22n	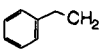	160	5.31
22o	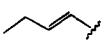	<100	4.94
22p		<100	4.85

3 indicates that branching and unsaturation in the *sn*-2 substituent reduce substrate activity by a larger amount than was expected from graphical examination of calculated structures.

Chemistry

The 1,2-dihexanoylglycerophospholipids **6a**–**g** were synthesized via the efficient synthesis of the phosphite triester resulting from coupling 1,2-dihexanoylglycerol with phenyldichlorophosphite followed by oxidation to the phosphate triester[17] (Scheme 1). This procedure provides an efficient route to a variety of phosphate head groups. It is necessary to purify the resulting phosphate diesters by flash chromatography through silica gel since the protecting groups cannot be removed by catalytic hydrogenolysis from the crude material.

The enantiomerically pure 1,2-bis(alkanoylthio)glycerophospholipids **12a**-**12g** were prepared by modification of published procedures[18] (Scheme 2). Commercially available (*R*)-(+)-glycidol is protected with *p*-anisylchlorodiphenylmethane and the resulting epoxide converted to the trithiocarbonate by heating with potassium hydroxide and carbon disulfide. The trithiocarbonate is easily recrystallized from ether–hexane. After lithium aluminum hydride reduction, the resulting thiol is immediately acylated with the acid chloride in hexane–pyridine. The protecting group is then removed and the phosphate head group introduced by standard procedures.

The 1-*O*-alkyl-2-(alkanoylthio)glycerophospholipids **22a**–**p** are prepared as shown in Scheme 3.[19]

Prolonged heating (~12–15 h) at 80–85 °C is required to produce 50–65% yields of the thioacetates **17**, which may be purified by flash chromatography. The thiol obtained upon reduction of the thioacetate is unstable and must be acylated immediately. The resulting thioesters **19** all perform well in the ensuing deprotection, phosphorylation, and demethylation steps denoted in Scheme 3.

It is noteworthy that removal of the 4-methoxytrityl (mmTr) protecting group does not lead to any sulfur to oxygen acyl migration under the acidic conditions shown for this step in Scheme 3. However, base does produce a rapid C_2 to C_3 acyl migration. In contrast, we have observed that mildly acidic removal of the mmTr group

Scheme 1

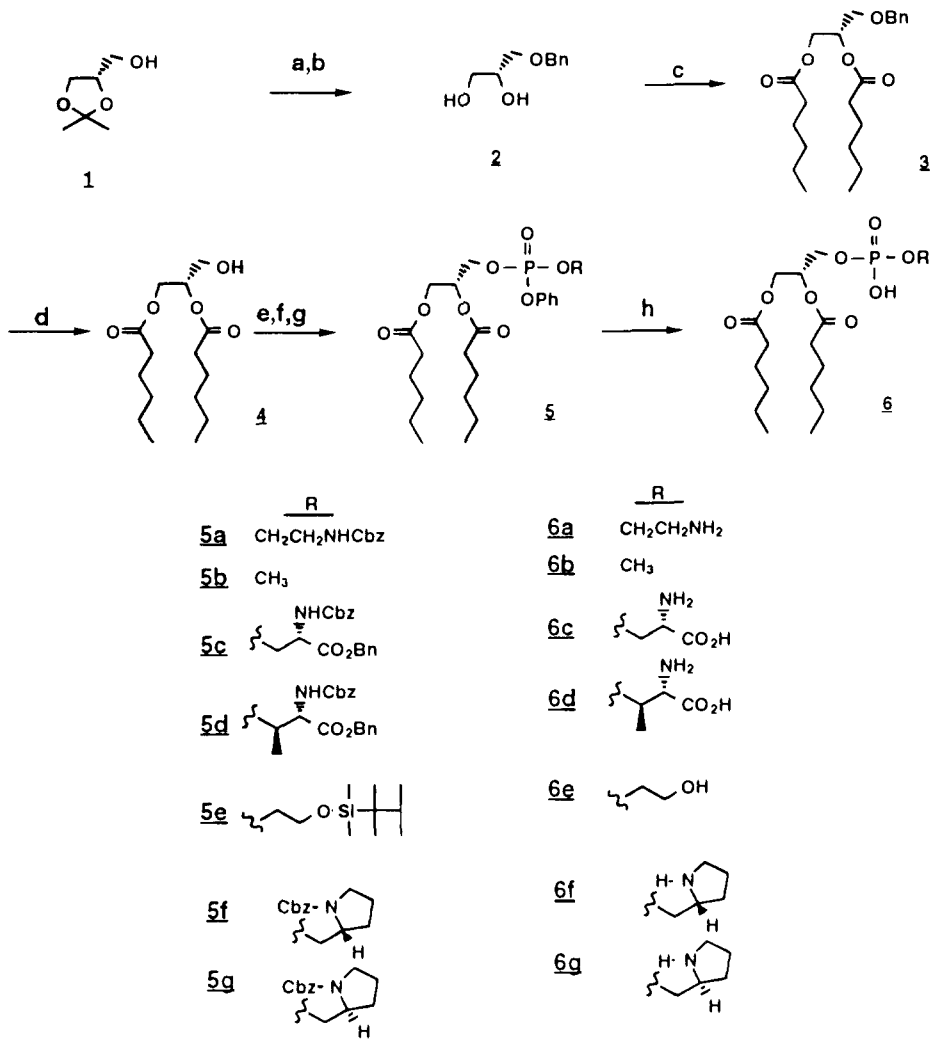

[a] Reagents: (a) NaH/DMF, BnBr; (b) HCl/CH_3OH-H_2O; (c) *n*-$C_5H_{11}COCl$, Et_3N, DMAP/CH_2Cl_2; (d) H_2/Pd$(OH)_2$/i-PrOH–HOAc (20:1); (e) $PhOPCl_2$/i-Pr_2NEt/THF, −78 °C; (f) ROH, −78 °C to room temperature; (g) $H_2O_2/CH_2Cl_2-H_2O$; (h) H_2, 10% Pd/C, PtO_2/HOAc–i-PrOH (for **5a,c,d,f,g**); H_2, PtO_2, HOAc–i-PrOH (for **5b**); $C_5H_5N(HF)_x$, THF then H_2, PtO_2, HOAc, i-PrOH for **5e**.

from 1-*O*-alkyl-2-alkanoylglyceryl 4-methoxytrityl ethers results in rapid C_2 to C_3 acyl migration.

Molecular Modeling

A model for hs-PLA_2 was constructed based on amino acid sequence similarity to bovine pancreatic[7] and *Crotalus atrox* venom PLA_2[8] using the programs Insight II, Homology, and Discover[20] and the program MVP.[21] The snake venom structure has greater sequence similarity and was thus used as the template. Since the snake venom structure is not complexed with calcium, the calcium binding loop was modeled by superimposing the bovine structure onto the snake venom structure, and then transplanting the calcium ion and residues A26 to A38 from the bovine structure into the snake venom template. Side chains were mutated as necessary to obtain the human sequence, and then adjusted into reasonable conformations by comparison to the available X-ray crystal structures.[7,8] Conformational search calculations were carried out on the side chains of Leu-2, His-6, and Lys-69 with the MVP program using a modified buildup procedure[21] adapted to use the CVFF force field.[22] The overall structure proved to be very similar to the subsequently-published X-ray structures of hs-PLA_2[8] and calcium- and ligand-bound hs-PLA_2.[9] The detailed structure within the active site region, including the side chain conformations, was in relatively good agreement with the calcium-bound hs-PLA_2 crystal structure.[9]

Although the structure of an amide substrate-based inhibitor bound to a pancreatic PLA_2 had been solved by X-ray crystallography,[10] the coordinates were not yet available at the time of this work. Consequently, published data from the study[10] was used to generate a model structure for the same inhibitor bound to hs-PLA_2. The compound was built and manually docked into the active site with Insight II,[20] using the published figures[10] as a guide. The initial structure was then refined by energy minimization with the CVFF force field,[22] using the published interatomic distances[10] as harmonic distance restraints with force constants of 5.0 kcal/Å^2. Prototype models for ester and thioester substrates were generated by converting the *sn*-2 amide nitrogen to either oxygen or sulfur, and then refining by energy minimization. The original default CVFF parameters gave a twisted thioester group. Semiempirical quantum calculations were carried out on model thioester compounds with the MOPAC program using the PM3 parameterization,[23] suggesting that the thioester preferred a trans conformation, with a barrier to rota-

Scheme 2

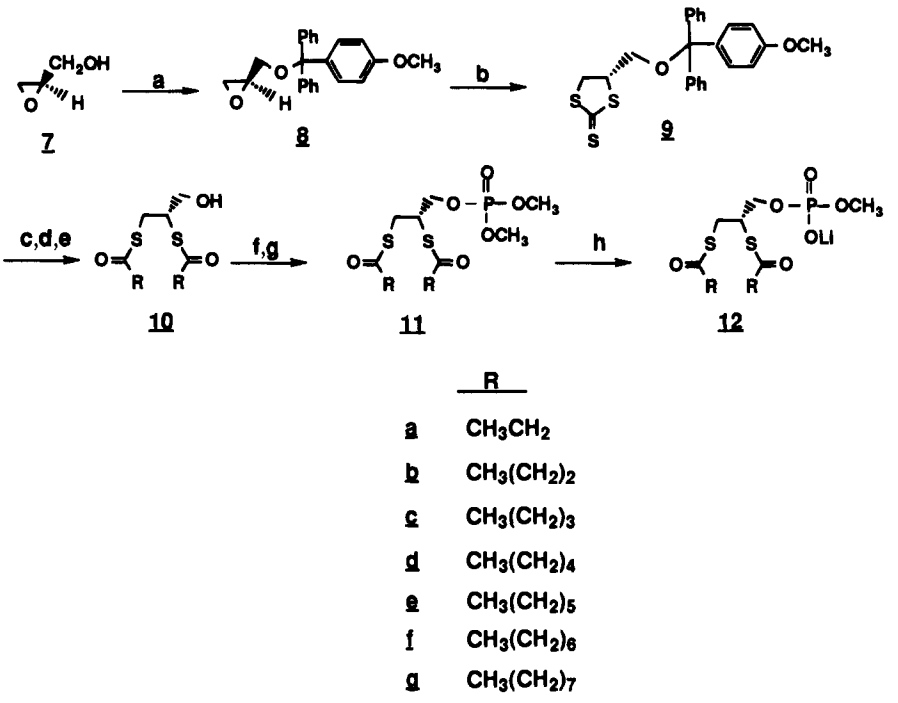

R	
a	CH_3CH_2
b	$CH_3(CH_2)_2$
c	$CH_3(CH_2)_3$
d	$CH_3(CH_2)_4$
e	$CH_3(CH_2)_5$
f	$CH_3(CH_2)_6$
g	$CH_3(CH_2)_7$

[a] Reagents: (a) mm–TrCl, TEA, $PhCH_3$, room temperature; (b) KOH, CS_2, MeOH, △; (c) LAH, Et_2O/THF; (d) RCOCl, pyr–hexane; (e) PTSA, 4:1 CH_2Cl_2–MeOH, room temperature, (f) $POCl_3$, TEA, 0 °C; (g) MeOH, TEA; (h) LiBr, MEK.

tion of 6.2 kcal. Examination of thioester structures in the Cambridge Crystallographic Database[24] suggested that a slightly higher barrier might be appropriate. Thus, the coefficient for the torsional potential in the CVFF force field for the thioester bond was set to −5.0 kcal, giving a calculated barrier to rotation of 9.0 kcal (after this work was completed, *ab initio* calculations were carried out with the Spartan program[25] at the 6-31G* level, using a model compound geometry optimized at the 3-21G* level, giving a barrier height of 10.7 kcal, in relatively good agreement with the parameterization used here). The resulting energy-minimized structures of straight-chain substrates bound to hs-PLA_2 were generally similar to the original X-ray structure,[10] as well as to the subsequently published structures of a phosphonate substrate-based inhibitor bound to cobra venom PLA_2[11] and hs-PLA_2.[9] Subsequent novel ester and thioester compounds were docked into the hs-PLA_2 model by superimposition onto corresponding atoms in the initial docked structure. Alternative conformations for the compounds were generated within the active site of the enzyme with the MVP program using a modified buildup procedure[21] adapted to use the CVFF force field.[22] The protein was held fixed during energy calculations except for the side chains of Leu-2, His-6, and Lys-69.

Conclusions

A series of short-chain phospholipid analogs having alkyl ether or oxy- or thioesters at the *sn*-1 position and oxy- or thioesters at the *sn*-2 position have been synthesized and used to examine the substrate specificity of human synovial fluid phospholipase A_2 by examining the rate of turnover of these substrates at concentrations well below the cmc of the substrate. Under these conditions the enzyme kinetics should reflect only the binding at the active site.

The 1,2-dihexanoyllglycerophospholipids were all turned over too slowly to be useful substrates. However, several of the 1,2-bis(alkanoylthio)- and 1-*O*-alkyl-2-(alkanoylthio)glycerophospholipids were hydrolyzed at reasonably high rates by hs-PLA_2 at concentrations well below their cmc. These compounds, e.g., **12d** and **22d**, have proven useful as monomeric substrates in an assay designed to identify active site inhibitors of hs-PLA_2.

Several structure–activity relationships for monomeric substrates of hs-PLA_2 have been found. Specific activity (k_{cat}/K_M) is linearly related to lipophilicity over a broad range of log *P* for compounds with straight chain substituents at the *sn*-1 and *sn*-2 positions. For comparable values of lipophilicity, the *sn*-1 ethers and *sn*-1 thioesters are turned over at similar rates. A negative charge in the phosphate head is necessary for substrate activity. Unsaturation, aromaticity, and branching in the *sn*-2 substituent reduce turnover dramatically. The same modifications in the *sn*-1 substituent have less effect on turnover.

In most cases, the experimental findings are consistent with expectations from the calculated structures. For example, the model clearly indicates that the *sn*-1 channel is wider and more open to solvent than the *sn*-2 channel. This is consistent with the experimental observation that chain branching, aromaticity, and double bonds are accommodated more easily in the *sn*-1 substituent than in the *sn*-2 substituent. Changes in the *sn*-1 substituent do, however, result in modification of substrate turnover. Thus, compound **22j**, which has an aromatic ring linked to the *sn*-1 oxygen by a three-carbon linker, has an activity similar to that of straight chain compounds with similar cLogP. In contrast, compounds **22g–i**, where the aromatic group is linked via a single methylene, have lower activity, suggesting a slightly poorer fit in the *sn*-1 channel. In addition, the *sn*-1 group in **22k** is substantially more bulky than

Scheme 3

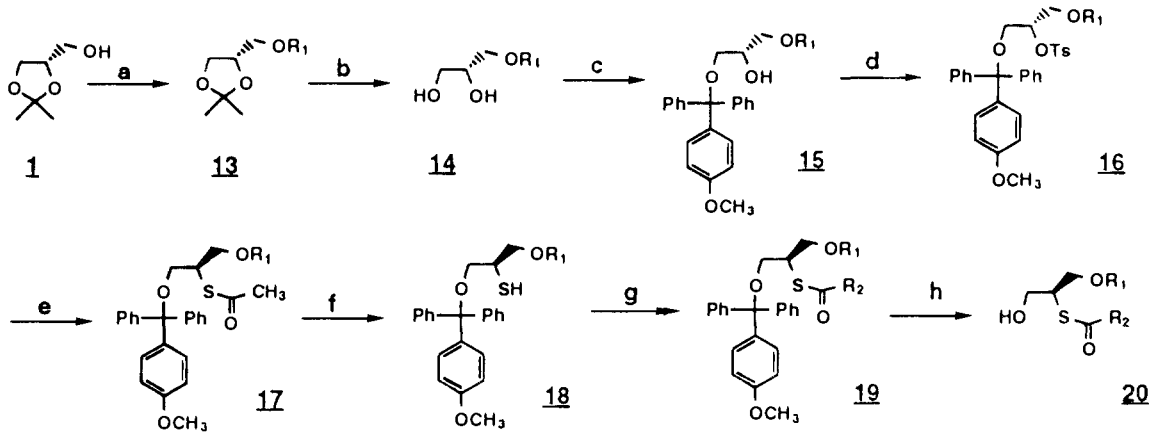

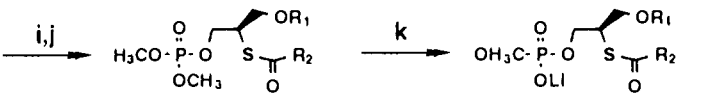

13-18		R_1
	a	$CH_3CH_2CH_2$
	b	$CH_3(CH_2)_4$
	c	$CH_3(CH_2)_5$
	d	$CH_3(CH_2)_7$
	e	$PhCH_2$
	f	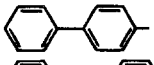
	g	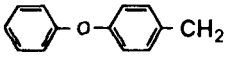
	h	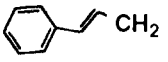
	i	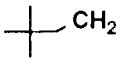
	j	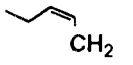

19-22		R_1	R_2
	a	$CH_3CH_2CH_2$	$CH_3CH_2CH_2$
	b	$CH_3(CH_2)_2$	$CH_3(CH_2)_6$
	c	$CH_3(CH_2)_4$	$CH_3(CH_2)_2$
	d	$CH_3(CH_2)_4$	$CH_3(CH_2)_6$
	e	$CH_3(CH_2)_7$	$CH_3(CH_2)_2$
	f	$CH_3(CH_2)_7$	$CH_3(CH_2)_6$
	g	$PhCH_2$	$CH_3(CH_2)_8$
	h	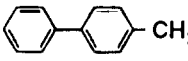	$CH_3(CH_2)_8$
	i	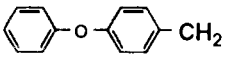	$CH_3(CH_2)_8$
	j	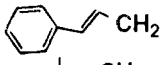	$CH_3(CH_2)_8$
	k	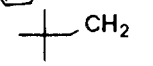	$CH_3(CH_2)_8$
	l	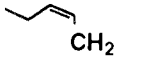	
	m	$CH_3(CH_2)_5$	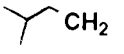
	n	$CH_3(CH_2)_5$	$PhCH_2CH_2$
	o	$CH_3(CH_2)_5$	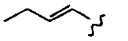
	p	$CH_3(CH_2)_5$	Ph

[a] Reagents: (a) NaH, R_1Br, DMF; (b) 9:1 MeOH: 1 N HCl; (c) MMTrCl, pyr–THF, 0 °C; (d) TsCl, pyr–CH_2Cl_2, 0 °C; (e) potassium thioacetate, DMF, 85 °C; (f) $NaBH_4$/EtOH, 50 °C; (g) R_2COCl, pyr, 0 °C; (h) PTSA, 4:1 CH_2Cl_2–MeOH; (i) $POCl_3$, TEA, 0 °C; (j) MeOH, TEA; (k) LiBr/MEK, room temperature.

the aromatic rings in **22g–i** and is substantially less active. Our results with **22g–i** are most interesting when compared to recently published work on a series of structurally related *inhibitors* of hs-PLA_2.[26]

None of the calculated protein–substrate structures showed any strong interaction that would preferentially stabilize an *sn*-1 ester or thioester. Some of the calculated structures had hydrogen bonds between the *sn*-1 ester or thioester and the side chain amino group of Lys-69. However, when this interaction occurred, it weakened the interaction with the phosphate head group. This lack of any strong interaction is consistent with the experimental finding that *sn*-1 ethers have approximately the same activity as *sn*-1 thioesters with comparable lipophilicity.

Both the X-ray and the model structures of hs-PLA_2 with bound ligand showed that the head group phosphate binds to the calcium and to the side-chain amino group of Lys-69. These two interactions should be strongest if the phosphate group has a full negative charge. This is consistent with the results in Table 4,

which demonstrate that a negative charge on the phosphate head group is necessary for substrate turnover.

Whereas the gross outlines of the experimental structure–activity relationships can be rationalized by examination of model structures, the finer details of the structure–activity relationship were not predicted and could not be rationalized. For example, the poor activity of compound **22o** was not expected. More sophisticated computational methodologies will be required to make quantitative predictions of activity.

Certain of these substrates, e.g., **12d**, have proven useful in assaying for active site inhibitors of hs-PLA_2. The structure–activity relationships defined for these short-chain substrates have assisted in the design of substrate analog inhibitors of hs-PLA_2.

Experimental Section

^1H NMR spectra were determined at 300 MHz on Varian Unity 300 or Varian VXR-300 insturments. Triethylamine, diisopropylamine, and diisopropylethylamine were distilled over calcium hydride prior to use. Anhydrous tetrahydrofuran, dichloromethane, diethyl ether, and toluene were purchased from Aldrich Chemical Co. and were used as received. All other solvents and reagents were purchased commercially and used as received. Flash column chromatography was performed on silica gel (EM Science, 230–400 mesh). Reverse-phase medium-pressure liquid chromatography (MPLC) was performed on C_{18} silica gel (Whatman LRP-2, 37–53 μm, 20 mm × 300 mm column) using a FMI model QSY pump. Elemental analyses were performed by Atlantic Microlab, Atlanta, GA. Thin-layer chromatography was conducted using silica gel (EM Science, Kieselgel 60 F_{254}) plates. Reverse-phase TLC was conducted using C_{18} (Whatman, $KC_{18}F$) plates.

Benzyl (2*R*)-2,3-Dihydroxy-1-propyl Ether (2). A slurry of 10.2 g (255 mmol) of 60% sodium hydride in oil was washed with hexane under nitrogen and was slurried in 300 mL of *N*,*N*-dimethylformamide under nitrogen. The mixture was chilled to 0 °C with stirring as 26.0 g (197 mmol) of (*S*)-2,3-isopropylideneglycerol (1) was added dropwise in 20 mL of *N*,*N*-dimethylformamide. After 30 min at 25 °C the mixture was chilled to 0 °C as 23.5 mL (198 mmol) of benzyl bromide was added dropwise. After 2 h at 0 °C and 2 h at 25 °C, the mixture was quenched carefully with water, diluted with more water, and extracted with two 200-mL portions of ethyl acetate. The pooled organics were washed with water and brine, and were dried over magnesium sulfate. Concentration in vacuo afforded 31.9 g of the crude benzyl ether: ^1H NMR ($CDCl_3$) δ 1.18 (s, 3H), 1.22 (s, 3H), 3.42 (dd, 1H), 3.54 (dd, 1H), 3.75 (dd, 1H), 4.07 (dd, 1H), 4.30 (m, 1H), 4.60 (d, 2H), 7.38 (m, 5H) ppm.

The above benzyl ether was diluted with 200 mL of methanol and treated with 2.5 mL of 5 N hydrochloric acid. After 2 h at reflux temperature the mixture was cooled to 25 °C and was concentrated in vacuo. Ether (200 mL) was added, the mixture was dried over magnesium sulfate and was concentrated in vacuo. The crude oil was chromatographed on 200 g of silica gel (elution with ether) to provide 25.1 g (70%) of the diol **2** as an oil: ^1H NMR ($CDCl_3$), δ 3.58 (d, 2H), 3.61 (dd, 1H), 3.70 (dd, 1H), 3.88 (m, 1H), 7.35 (m, 5H) ppm.

Benzyl (2*S*)-2,3-Bis(hexanoyloxy)-1-propyl Ether (3). A solution of 18.0 g (98.8 mmol) of glycerol derivative **2** in 300 mL of dichloromethane was stirred at 0 °C as 35.0 mL (251 mmol) of triethylamine and 1 g of 4-(dimethylamino)pyridine was added, followed by dropwise addition of 31.6 mL (221 mmol) of hexanoyl chloride. After 6 h at 25 °C, the mixture was quenched by addition of 20 mL of *N*,*N*-dimethylethylenediamine. Water was added, and the mixture was concentrated to a volume of 100 mL. The residue was further diluted with water and was extracted with two 200-mL portions of ethyl acetate. The organics were washed with saturated aqueous sodium bicarbonate, water, 1 N sulfuric acid, and brine and were dried over magnesium sulfate. Concentration in vacuo followed by chromatography of the crude material on 200 g of silica gel (elution with 30% ethyl acetate–hexane) gave 31.31 g (84%) of the diester **3** as an oil: ^1H NMR ($CDCl_3$) δ 0.85 (bt, 6H), 1.30 (m, 8H), 2.23 (t, 2H), 2.30 (t, 2H), 3.60 (d, 2H), 4.20 (dd, 1H), 4.37 (dd, 1H), 4.57 (AB q, 2H), 5.23 (m, 1H), 7.38 (m, 5H) ppm.

(2*S*)-1,2-Bis(hexanoyloxy)-1-propanol (4). A solution of 5.00 g (13.20 mmol) of the benzyl ether **3** in 50 mL of 2-propanol and 5 mL of acetic acid was added to 750 mg of 10% palladium hydroxide on carbon in a pressure bottle under nitrogen. The mixture was shaken under 50 psi of hydrogen for 18 h. The mixture was then filtered, and the filtrate was concentrated under reduced pressure. Purification of the crude product by medium-pressure liquid chromatography (40 × 300 mm silica gel column, 20% ethyl acetate/hexane) gave 3.22 g (85%) of the title compound as an oil: ^1H NMR ($CDCl_3$) δ 0.84 (bt, 6H), 1.30 (m, 8H), 1.61 (m, 4H), 2.31 (t, 2H), 2.35 (t, 2H), 3.72 (d, 2H), 4.22 (dd, 1H), 4.32 (dd, 1H), 5.07 (m, 1H) ppm.

General Procedure for the Preparation of the Unsymmetrical Phosphates 5a–g. A solution of 1.5–2.5 mmol of phenyl dichlorophosphite in tetrahydrofuran (0.5 M) was chilled to −78 °C under nitrogen and was treated with *N*,*N*-diisopropylethylamine (4 equiv). A solution of (2*S*)-1,2-bis-(hexanoyloxy)-1-propanol (**4**) (1.0 equiv) in 1 mL of tetrahydrofuran was added dropwise. After 15 min at −78 °C the second alcohol component (1.3 equiv) in 1–2 mL of tetrahydrofuran was added. The mixture was allowed to stir at −78 °C for 1 h, then warmed to 25 °C, and kept thusly for 14 h. The reaction mixture was diluted with 30–50 mL of ethyl acetate and was filtered through Celite. The filtrate was concentrated under reduced pressure to provide the crude phenyl phosphite, which was not characterized or purified but directly oxidized to the phenyl phosphate by addition of 30% hydrogen peroxide (1 mL/mmol of $PhOPCl_2$ employed) to a stirring solution of the crude phosphite in dichloromethane (0.1–0.2 M). After 1–4 h, the organic layer was separated, dried over magnesium sulfate, and concentrated in vacuo. Purification by chromatography afforded the mixed phosphates.

2-[(Benzyloxycarbonyl)amino]ethyl (2*R*)-1,2-bis(hexanoyloxy)-1-propyl phenyl phosphate (5a) [chromatography on silica gel/30% ethyl acetate–hexane; 70% ethyl acetate–hexane]: yield 52%; oil; ^1H NMR ($CDCl_3$) δ 0.83 (bt, 6H), 1.22 (bs, 8H), 1.60 (bs, 4H), 2.23 (m, 4H), 3.48 (bs, 2H), 4.18 (m, 2H), 4.22 (m, 4H), 5.10 (s, 2H), 5.14 (m, 1H), 5.38 (bs, 1H), 7.20 (bs, 4H), 7.39 (bs, 6H) ppm.

(2*R*)-1,2-Bis(hexanoyloxy)-1-propyl methyl phenyl phosphate (5b) [chromatography on silica gel/20% ethyl acetate–hexane; 50% ethyl acetate–hexane]: yield 61%; oil; 1H NMR ($CDCl_3$) δ 0.82 (bt, 6H), 1.24 (bs, 8H), 1.60 (bs, 4H), 2.32 (m, 4H), 3.82 and 3.92 (2 d, 3H), 4.19 (m, 2H), 4.30 (m, 4H), 5.13 (m, 1H), 7.10 (m, 3H), 7.20 (m, 2H) ppm.

(1*S*)-1-[(Benzyloxycarbonyl)amino]-1-(benzyloxycarbonyl)-2-ethyl (2*R*)-1,2-bis(hexanoyloxy)-1-propyl phenyl phosphate (5c) [chromatography on silica gel/30% ethyl acetate–hexane; 50% ethyl acetate–hexane]: yield 58%; oil; ^1H NMR ($CDCl_3$) δ 0.82 (m, 6H), (1.23 (m, 8H), 1.60 (m, 4H), 2.23 (m, 4H), 4.20 (m, 6H), 4.60 (m, 1H), 5.10 and 5.19 (m, 4H), 5.21 (m, 1H), 5.78 and 5.90 (2 d, 1H), 7.19 (m, 2H), 7.37 (m, 13H) ppm.

(1*S*,2*R*)-1-[(Benzyloxycarbonyl)amino]-1-(benzyloxycarbonyl)-2-propyl (2*R*)-1,2-bis(hexanoyloxy)-1-propyl phenyl phosphate (5d) [chromatography on silica gel/30% ethyl acetate–hexane]: yield 62%; oil; ^1H NMR ($CDCl_3$) δ 0.83 (bs, 6H), 1.28 (bs, 8H), 1.42 (2 d, 3H), 1.62 (m, 4H), 2.25 (m, 4H), 4.20 and 4.52 (m, 5H), 4.82 (m, 1H), 5.09 (m, 5H), 5.62 and 5.78 (2 d), 7.18 (m, 2H), 7.38 (m, 13H) ppm.

(2*R*)-1,2-Bis(hexanoyloxy)-1-propyl phenyl 2-[[(1,1,2-trimethylpropyl)dimethylsilyl]oxy]ethyl phosphate (5e) [chromatography on silica gel/20% ethyl acetate–hexane; 70% ethyl acetate–hexane]: yield 55%; oil; ^1H NMR ($CDCl_3$) δ 0.10 (s, 6H), 0.82 (m, 13H), 0.85 (m, 6H), 1.30 (m, 8H), 1.61 (m, 4H), 2.28 (m, 4H), 3.80 (bt, 2H), 4.18 and 4.30 (bm, 6H), 5.22 (m, 1H), 7.20 (m, 3H), 7.38 (m, 2H) ppm.

[(2*R*)-1-(Benzyloxycarbonyl)pyrrolidin-2-yl]methyl (2*R*)-1,2-bis(hexanoyloxy)-1-propyl phenyl phosphate (5f) [chro-

matography on silica gel/30% ethyl acetate–hexane; 40% ethyl acetate–hexane; 50% ethyl acetate–hexane]: yield 65%; oil; ^{1}H NMR ($CDCl_3$) δ 0.90 (m, 6H), 1.32 (m, 8H), 1.62 (m, 4H), 1.83 and 1.97 (2 m), 2.31 and 3.40 (2 m, 2H), 4.10 and 4.25 (2 m, 7H), 5.11 (m, 2H), 5.23 (m, 1H), 7.21 (m, 3H), 7.39 (m, 7H) ppm.

[(2*S*)-1-(Benzyloxycarbonyl)pyrrolidin-2-yl]methyl (2*R*)-1,2-bis(hexanoyloxy)-1-propyl phenyl phosphate (5g) [chromatography on silica gel/20% ethyl acetate–hexane; 40% ethyl acetate–hexane; 50% ethyl acetate–hexane]: yield 62%; oil; ^{1}H NMR ($CDCl_3$) δ 0.88 (m, 6H), 1.33 (m, 8H), 1.60 (m, 4H), 1.81 and 1.95 (2 m), 2.30 (m, 4H), 3.40 (m, 2H), 4.05 and 4.25 (2 m, 7H), 5.08 (m, 2H), 5.20 (m, 1H), 7.18 (m, 3H), 7.38 (m, 7H) ppm.

(2*R*)-1,2-Bis(hexanoyloxy)-1-propyl 2-Hydroxyethyl Phenyl Phosphate. The phosphate 5e (505 mg, 0.86 mmol) was stirred in 2 mL of tetrahydrofuran at 0 °C as 0.75 mL of 70% hydrogen fluoride–pyridine was added. The mixture was warmed to 25 °C after 1 h, and another 0.75 mL aliquot of hydrogen fluoride–pyridine was added. After an additional hour the mixture was diluted with 50 mL of ethyl acetate and was washed with water and brine. Drying of the organic phase over magnesuim sulfate and concentration in vacuo gave the crude product which was chromatographed on 25 g of silica gel (elution with 50% ethyl acetate–hexane followed by 70% ethyl acetate–hexane) to provide 204 mg (52%) of the phenyl hydroxyethyl phosphate as an oil: ^{1}H NMR ($CDCl_3$) δ 0.88 (bs, 6H), 1.30 (bs, 8H), 1.61 (m, 4H), 2.35 (m, 4H), 3.83 (bs, 2H), 4.20 and 4.30 (2 m, 6H), 5.25 (m, 1H), 7.21 (m, 3H), 7.40 (m, 2H) ppm.

(2*R*)-1,2-Bis(hexanoyloxy)-1-propyl 2-Hydroxyethyl Phosphate (6e). The phenyl phosphate from the above step was treated with 100 mg of platinum oxide, and the mixture was diluted with 2 mL of acetic acid and 2 mL of 2-propanol. The mixture was stirred under a balloon of hydrogen gas for 2 h at 25 °C. The mixture was filtered, and the filtrate was concentrated under reduced pressure to give the crude product, which was purified by chromatography on silica gel (elution with chloroform followed by 60:35:5 chloroform/methanol/water) to provide 117 mg (73%) of the phosphoglycerol derivative 7e as a viscous oil: ^{1}H NMR ($CDCl_3$) δ 0.85 (bs, 6H), 1.28 (m, 8H), 2.29 (m, 4H), 3.70 (bs, 2H), 3.95 (m, 4H), 4.18 (m, 2H), 5.23 (m, 2H) ppm. Anal. ($C_{17}H_{33}O_9P\cdot0.5H_2O$) C, H.

(2*R*)-1,2-Bis(hexanoyloxy)-1-propyl Methyl Phosphate (6b). A mixture of 258 mg (0.563 mmol) of phenyl phosphate 5b in 3 mL of acetic acid and 3 mL of 2-propanol was added to 150 mg of platinum oxide. The mixture was stirred under a balloon of hydrogen gas for 4 h, at which time the mixture was filtered and the filtrate was concentrated. Chromatography of the residue on silica gel (elution with chloroform followed by 60:35:5 chloroform/methanol/water) gave 156 mg (72%) of the phosphate as a waxy solid: ^{1}H NMR ($CDCl_3$) δ 0.88 (bs, 6H), 1.30 (bs, 8H), 1.58 (bs, 4H), 2.27 (m, 4H), 3.60 (d, 3H), 4.00 (bs, 2H), 4.20 bs, 2H), 5.21 (m, 1H) ppm; MS *m/e* [M − 1] 381. Anal. ($C_{16}H_{31}O_8P\cdot0.5\ H_2O$) C, H.

General Procedure: Deprotection of Mixed Phosphates 5a, 5c, 5d, 5f, and 5g. The phenyl phosphate in 1:1 2-propanol/acetic acid (0.1 M) was added to a mixture of platinum oxide (0.5 g/g of phosphate) and 10% palladium on carbon (1 g/g of phosphate) under nitrogen. The mixture was rapidly stirred under a balloon of hydrogen gas for 4–12 h or generally until thin-layer chromatography indicated no remaining material absorbing at 254 nm. The mixture was filtered, and the filtrate was concentrated in vacuo. The crude product was purified by chromatography on silica gel.

2-Aminoethyl (2*R*)-1,2-bis(hexanoyloxy)-1-propyl phosphate (6a) [chromatography on silica gel/chloroform; 60:35:5 chloroform/methanol/water]: yield 75%; waxy solid; ^{1}H NMR ($CDCl_3$) δ 0.86 (m, 6H), 1.30 (m, 8H), 1.63 (m, 4H), 2.28 (2 t, 4H), 3.19 (bs, 2H), 3.97 (m, 2H), 4.18 (m, 2H), 4.16 (dd, 1H), 4.20 (dd, 1H), 5.21 (m, 1H) ppm; MS *m/e* [M − 1] 410. Anal. ($C_{17}H_{34}NO_8P\cdot0.25\ H_2O$) C, H, N.

(1*S*)-1-Amino-1-carboxy-2-ethyl (2*R*)-1,2-bis(hexanoyloxy)-1-propyl Phosphate (6c) [chromatography on silica gel/chloroform; 60:35:5 chloroform/methanol/water]: yield 85%; waxy solid; ^{1}H NMR ($CDCl_3$) δ 0.85 (bs, 6H), 1.31 (bs, 8H), 1.60 (bs, 4H), 2.29 (bs, 4H), 3.98 (m, 2H), 4.18 (m, 3H), 4.38 (m, 2H), 5.22 (m, 1H) ppm. Anal. ($C_{18}H_{34}NO_{10}P\cdot0.25H_2O$) C, H; N: calcd, 3.05; found, 2.62.

(1*S*,2*R*)-1-Amino-1-carboxy-2-propyl (2*R*)-1,2-bis(hexanoyloxy)-1-propyl phosphate (6d) [chromatography on silica gel/chloroform; 60:35:5 chloroform/methanol/water]: yield 62%; waxy solid; ^{1}H NMR ($CDCl_3$) δ 0.88 (bs, 6H), 1.36 (bs, 11H), 1.58 (bs, 4H), 2.23 (bs, 4H), 3.97 (m, 2H), 4.16 (m, 3H), 4.40 (m, 2H), 5.23 (m, 1H) ppm. Anal. ($C_{19}H_{36}NO_{10}P\cdot1.0H_2O$) C, H, N.

(2*R*)-1,2-Dihexanoyl-1-propyl [(2*R*)-1-pyrrolidin-2-yl]-methyl phosphate (6f) [chromatography on silica gel/chloroform; 60:35:5 chlolroform/methanol/water]: yield 61%; waxy solid; ^{1}H NMR ($CDCl_3$) δ 0.90 (t, 6H), 1.37 (bs, 8H), 1.60 (bs, 4H), 1.71 (m, 1H), 2.03 (m, 3H), 2.37 (m, 4H), 3.33 (bs, 2H), 3.83 (bs, 1H), 4.00 (m, 2H), 4.10 (m, 1H), 4.18 (dd, 1H), 4.39 (dd, 1H), 5.21 (bs, 1H) ppm; MS *m/e* [M − 1] 450. Anal. ($C_{20}H_{38}NO_8P\cdot0.5H_2O$) C, H, N.

(2*R*)-1,2-Bis(hexanoyloxy)-1-propyl [(2*S*)-1-pyrrolidin-2-yl]methyl phosphate (6g) [chromatography on silica gel/chloroform; 60:35:5 chlolroform/methanol/water]: yield 62%; waxy solid; ^{1}H NMR ($CDCl_3$) δ 0.88 (t, 6H), 1.36 (bs, 8H), 1.61 (bs, 4H), 2.03 (m, 2H), 2.33 (m, 4H), 3.25 (bt, 2H), 3.86 (bs, 1H), 4.00 (m), 4.10 (m, 1H), 4.18 (dd, 1H), 4.40 (dd, 1H), 5.22 (m, 1H) ppm; MS *m/e* [M − 1] 450. Anal. ($C_{20}H_{38}NO_8P\cdot1.0H_2O$) C, H, N.

(2*S*)-3-[[(4-Methoxyphenyl)diphenylmethyl]oxy]-1,2-propylene-Trithiocarbonate (9). A mixture of the epoxide 8 (15.17 g, 43.8 mmol), potassium hydroxide (14.99 g, 267.1 mmol), and carbon disulfide (24.0 g, 315.3 mmol) in methanol (100 mL) was heated at reflux for 2 h. The mixture was then poured into water and was extracted with dichloromethane. The organic phases were dried over magnesium sulfate and concentrated in vacuo to a yellow oil. Crystallization from 10% hexane in ether and collection by filtration afforded the product (9.7 g, 57%) as a yellow solid: ^{1}H NMR (acetone-d_6) δ 3.45–3.60 (m, 2H), 3.80 (s, 3H), 4.05–4.30 (m, 2H), 4.70–4.85 (m, 1H), 6.85–7.55 (m, 14H) ppm.

General Procedure: (2*S*)-2,3-Bis(hexanoylthio)-1-propyl (4-Methoxyphenyl)diphenylmethyl Ether. To a stirred slurry of lithium aluminum hydride (839 mg, 22.1 mmol) in anhydrous diethyl ether (50 mL) was added a solution of the above trithiocarbonate (9.70 g, 22.1 mmol) in tetrahydrofuran (75 mL) over 1 h. The reaction mixture was stirred at 25 °C for 1 h and then cooled in an ice bath. The reaction was quenched by the dropwise addition of water (50 mL), adjusted to pH 4.0 with 1 N hydrochloric acid, and extracted with ether. The ether was washed with water, saturated aqueous sodium bicarbonate, and water. The combined organic phases were dried over magnesium sulfate and concentrated in vacuo to afford the crude dithiol. To a solution of the dithiol in 25% pyridine–hexane (100 mL) at 0 °C was added dropwise a solution of hexanoyl chloride (8.93 g, 66.3 mmol) in hexane (10 mL). The reaction mixture stirred 14 h at 25 °C. The mixture was partitioned between ether and water. The organic phase was washed with water, dried over magnesium sulfate, and concentrated. The residue was chromatographed on silica gel (elution with 10% ethyl acetate in hexane) to afford the desired product (6.95 g, 53%) as an oil: H NMR (acetone-d_6) δ 0.80–0.95 (m, 6H), 1.25–1.40 (m, 8H), 1.50–1.70 (m, 4H), 2.50–2.65 (m, 4H), 3.20–3.45 (m, 4H), 3.80 (s, 3H), 3.85–3.95 (m, 1H), 6.85–7.55 (m, 14H) ppm.

(2*S*)-2,3-Bis(hexanoylthio)-1-propyl Dimethyl Phosphate (11d). A mixture of the above dithioester (6.90 g, 11.6 mmol) and *p*-toluenesulfonic acid (15 mg) in dichloromethane/methanol (80 mL/20 mL) was stirred at 25 °C for 1 h. Pyridine (1 mL) was added, and the reaction mixture was concentrated. The residue was taken up in ether (60 mL) and filtered. The filtrate was concentrated and placed under high vacuum for 1 h to afford the crude alcohol. To a solution of phosphorus oxychloride (2.14 g, 14.0 mmol) and triethylamine (2.12 g, 21.0 mmol) in tetrahydrofuran (10 mL) at 0 °C was added dropwise a solution of the crude alcohol in tetrahydrofuran (20 mL). The reaction stirred at 0 °C for 45 min, and then a solution of methanol (8 mL) and triethylamine (6 mL) was added dropwise. The reaction was stirred at 25 °C for 14 h. The reaction

mixture was diluted with ether (25 mL) and filtered. The filtrate was concentrated, and the residue was chromatographed on silica gel (elution with 50% ethyl acetate–hexane) to afford the product **11d** as an oil (2.95 g, 59%): ^{1}H NMR ($CDCl_3$) δ 0.80–0.95 (m, 6H), 1.20–1.40 (m, 8H), 1.55–1.70 (m, 4H), 2.55 (t, 4H), 3.10–3.40 (m, 2H), 3.75 (d, 6H), 3.80–3.90 (m, 1H), 4.00–4.30 (m, 2H) ppm.

Lithium (2*S*)-2,3-Bis(hexanoylthio)-1-propyl Methyl Phosphate (12d). A mixture of the above dimethyl phosphate **11d** (3.82 g, 8.90 mmol) and lithium bromide (2.32 g, 26.7 mmol) in 2-butanone (35 mL) was stirred at 25 °C for 14 h. The reaction mixture was concentrated and the residue purified by reverse-phase chromatography (acetonitrile:methanol:water; 2:2:1) to afford the desired product **13d** as a white solid (3.62 g, 96%): ^{1}H NMR (DMSO-d_6) δ 0.85 (t, 6H), 1.17–1.32 (m, 8H), 1.47–1.60 (m, 4H), 2.50–2.60 (m, 4H), 3.02–3.12 (m, 1H), 3.25–3.35 (m, 4H), 3.60–3.80 (m, 3H) ppm. Anal. ($C_{16}H_{30}LiO_6PS$) C, H, S.

Lithium (2*S*)-2,3-bis(propanoylthio)-1-propyl methyl phosphate (12a): ^{1}H NMR (DMSO-d_6) δ 1.06 (t, 3H), 1.07 (t, 3H), 2.60 (q, 2H), 2.61 (q, 2H), 3.11 (dd, 1H), 3.27 (dd, 1H), 3.32 (d, 3H), 3.6–3.8 (m, 3H). Anal. ($C_{10}H_{18}O_6PS_2Li$) C, H, S.

Lithium (2*S*)-2,3-bis(butanoylthio)-1-propyl methyl phosphate (12b): ^{1}H NMR (DMSO-d_6) δ 0.89 (t, 6H), 1.54–1.63 (m, 4H), 2.53–2.58 (m, 4H), 3.10 (dd, 1H), 3.30 (dd, 1H), 3.31 (d, 3H), 3.6–3.8 (m, 3H). Anal. ($C_{12}H_{22}O_6PS_2Li$) C, H, S.

Lithium (2*S*)-2,3-bis(pentanoylthio)-1-propyl methyl phosphate (12c): ^{1}H NMR (DMSO-d_6) δ 0.87 (t, 6H), 1.25–1.34 (m, 4H), 1.51–1.58 (m, 4H), 2.55–2.60 (m, 4H), 3.09 (dd, 1H), 3.29 (dd, 1H), 3.31 (d, 3H), 3.6–3.8 (m, 3H). Anal. ($C_{14}H_{26}O_6PS_2Li$) C, H, S.

Lithium (2*S*)-2,3-bis(heptanoylthio)-1-propyl methyl phosphate (12e): ^{1}H NMR (DMSO-d_6) δ 0.86 (t, 6H), 1.21–1.31 (m, 12H), 1.51–1.58 (m, 4H), 2.54–2.58 (m, 4H), 3.09 (dd, 1H), 3.30 (dd, 1H), 3.33 (d, 3H), 3.6–3.8 (m, 3H). Anal. ($C_{18}H_{34}O_6PS_2Li$) C, H, S.

Lithium (2*S*)-2,3-bis(octanoylthio)-1-propyl methyl phosphate (12f): ^{1}H NMR (DMSO-d_6) δ 0.85 (t, 6H), 1.20–1.30 (m, 16H), 1.51–1.58 (m, 4H), 2.54–2.58 (m, 4H), 3.09 (dd, 1H), 3.30 (dd, 1H), 3.33 (d, 3H), 3.6–3.8 (m, 3H). Anal. ($C_{20}H_{38}O_6PS_2Li$) C, H, S.

Lithium (2*S*)-2,3-bis(nonanoylthio)-1-propyl methyl phosphate (12g): ^{1}H NMR (DMSO-d_6) δ 0.85 (t, 6H), 1.19–1.29 (m, 20H), 1.51–1.58 (m, 4H), 2.54–2.58 (m, 4H), 3.09 (dd, 1H), 3.30 (dd, 1H), 3.33 (d, 3H), 3.6–3.8 (m, 3H). Anal. ($C_{22}H_{42}O_6PS_2Li$) C, H, S.

General Procedure: (2*S*)-1-*O*-Hexyl-2,3-*O*-isopropylideneglycerol (13c). To a stirred slurry of sodium hydride (4.54 g, 113.5 mmol) in *N*,*N*-dimethylformamide (50 mL) was added dropwise (2*S*)-1,2-*O*-isopropylideneglycerol (10.0 g, 75.6 mmol) in *N*,*N*-dimethylformamide (50 mL) (gas evolution). The reaction mixture was stirred for 45 min. 1-Bromohexane (15.20 g, 92.0 mmol) in *N*,*N*-dimethylformamide (50 mL) was added dropwise, and the reaction mixture was stirred at 25 °C for 14 h. The reaction mixture was poured into ice water (250 mL), extracted with ether, dried over magnesium sulfate, and concentrated. The residue was chromatographed on silica gel (elution with 10% ethyl acetate in hexane) to afford the product (14.12 g, 87%) as a liquid: ^{1}H NMR ($CDCl_3$) δ 0.90 (t, 3H), 1.20–1.38 (m, 6H), 1.40 (d, 6H), 1.50–1.65 (m, 2H), 3.35–3.58 (m, 4H), 3.70–3.78 (m, 1H), 4.02–4.10 (m, 1H), 4.20–4.30 (m, 1H) ppm.

(2*S*)-3-(Hexyloxy)-1,2-propanediol (14c). To a stirred solution of the above isopropylideneglycerol (12.30 g, 56.9 mmol) in methanol (150 mL) was added dropwise 1 N hydrochloric acid (20 mL), and the mixture was stirred at 25 °C for 24 h. The reaction mixture was concentrated, taken up in benzene (250 mL), and concentrated again. Trace solvent was removed under high vacuum to afford the desired diol (10.00 g, quant): ^{1}H NMR ($CDCl_3$) δ 0.88 (t, 3H), 1.20–1.60 (m, 6H), 1.50–1.65 (m, 2H), 2.30–2.50 (br, 2H), 3.40–3.80 (m, 7H) ppm.

(2*S*)-1-(Hexyloxy)-3-[(4-methoxyphenyl)diphenylmethoxy]-2-propanol (15c). To a stirred solution of the above diol (10.00 g, 56.7 mmol) in pyridine (100 mL) at 0 °C was added dropwise a solution of *p*-anisylchlorodiphenylmethane (21.02 g, 68.1 mmol) in tetrahydrofuran (60 mL). The mixture was allowed to come to 25 °C and stir for 14 h. The reaction mixture was concentrated and partitioned between ether (200 mL) and water (200 mL). The ether layer was washed with water, dried over magnesium sulfate, and concentrated. The residue was chromatographed on silica gel (elution with 20% ethyl acetate in hexane) to afford the product (23.65 g, 92%) as a yellow gum: ^{1}H NMR (acetone-d_6) δ 0.90 (t, 3H), 1.20–1.38 (m, 6H), 1.42–1.55 (m, 2H), 3.10–3.20 (m, 2H), 3.38–3.58 (m, 4H), 3.78–3.95 (m, 4H), 6.85–7.55 (m, 14H) ppm.

(2*S*)-1-(Hexyloxy)-3-[(4-methoxyphenyl)diphenylmethoxy]-2-propyl *p*-Toluenesulfonate (16c). To a stirred solution of the above alcohol **15c** (23.60 g, 52.6 mmol) in pyridine (120 mL) at 0 °C was added dropwise a solution of *p*-toluenesulfonyl chloride (25.07 g, 131.5 mmol) in dichloromethane (60 mL). The mixture was stirred at 25 °C for 14 h. The reaction mixture was concentrated and partitioned between ether (300 mL) and water (300 mL). The ether layer was washed with water, and the organic phase was dried over magnesuim sulfate. The organic phase was concentrated under reduced pressure, and the residue was chromatographed on silica gel (elution with 15% ethyl acetate in hexane) to afford the product (22.50 g, 71%) as an oil: ^{1}H NMR (acetone-d_6) δ 0.90 (t, 3H), 1.15–1.42 (m, 8H), 2.42 (s, 3H), 3.20–3.35 (m, 4H), 3.50–3.68 (m, 2H), 3.80 (s, 3H), 3.65–3.75 (m, 1H), 6.82–7.85 (m, 18H) ppm.

(2*R*)-1-(Hexyloxy)-3-[(4-methoxyphenyl)diphenylmethoxy]-2-propyl Thioacetate (17c). The above tosylate **16c** (22.50 g, 37.3 mmol) in *N*,*N*-dimethylformamide (80 mL) was added dropwise to a stirred solution of potassium thioacetate (8.53 g, 74.6 mmol) in *N*,*N*-dimethylformamide (80 mL). The mixture was heated at 80 °C for 16 h. The reaction mixture was concentrated and taken up in ether (300 mL). The ether layer was washed with water, dried over magnesium sulfate, and concentrated in vacuo. The residue was chromatographed on silica gel (elution with 10% ethyl acetate in hexane) to afford the product (13.25 g, 70%) as a yellow gum: ^{1}H NMR (acetone-d_6) δ 0.88 (t, 3H), 1.20–1.37 (m, 6H), 1.40–1.55 (m, 2H), 2.32 (s, 3H), 3.20–3.45 (m, 4H), 3.63–3.70 (m, 2H), 3.80 (s, 3H), 3.82–3.92 (m, 1H), 6.83–7.50 (m, 14H) ppm.

(2*R*)-1-(Hexyloxy)-3-[(4-methoxyphenyl)diphenylmethoxy]-2-propanethiol (18c). A solution of the above thioacetate **17c** (7.60 g, 15.0 mmol) in absolute ethanol (100 mL) was heated to 55 °C. Sodium borohydride (5.00 g, 132.2 mmol) was added portionwise and mixture heated at 55 °C for 1 h. The reaction mixture was poured into ice water (500 mL), extracted with ether, dried over magnesium sulfate, and concentrated in vacuo to afford the thiol (6.90g, 100%): ^{1}H NMR (acetone-d_6) δ 0.88 (t, 3H), 1.20–1.38 (m, 6H), 1.45–1.55 (m, 2H), 3.05–3.15 (m, 1H), 3.25–3.70 (m, 6H), 3.80 (s, 3H), 6.83–7.50 (m, 14H) ppm.

(2*R*)-1-(Hexyloxy)-3-[(4-methoxyphenyl)diphenylmethoxy]-2-propyl Thiobenzoate (19p). To a stirred solution of the above thiol **18c** (1.72 g, 3.7 mmol) in pyridine (5 mL) at 0 °C was added benzoyl chloride (0.79 g, 5.6 mmol). The reaction was stirred at 25 °C for 14 h. The reaction mixture was poured into ice water and was extracted with ether. The organic phases were dried over magnesium sulfate and were concentrated under reduced pressure. The residue was chromatographed on silica gel (elution with 10% ethyl acetate in hexane) to afford the product (1.40 g, 67%) as a light yellow oil: ^{1}H NMR (acetone-d_6) δ 0.88 (t, 3H), 1.20–1.38 (m, 6H), 1.45–1.55 (m, 2H), 3.30–3.53 (m, 4H), 3.75–3.85 (m, 5H), 4.10–4.20 (m, 1H), 6.83–8.00 (m, 19H) ppm.

General Procedure: Detritylation, Phosphorylation, and Dealkylation of 19a–f. The protected alcohol **19** was dissolved in 2:1 methanol/toluene. Amberlite IR-120(plus) (H form) was added and the mixture was stirred at 25 °C for 5 h. The mixture was filtered to remove the resin, and the filtrate was concentrated in vacuo. The residue was chromatographed on silica gel (elution with 10% ethyl acetate–hexanes followed by 20% ethyl acetate–hexanes) to provide the alcohols **20a–f**. These compounds were phosphorylated via the phosphite

triester method using methyl dichlorophosphite according to the procedure denoted in Scheme 1. The dimethyl phosphates **21a–f** were dealkylated according to the procedure in Scheme 2 to give **22a–f** after reverse-phase liquid chromatography.

Lithium methyl (2*R*)-3-(propyloxy)-2-(butanoylthio)-1-propyl phosphate (22a): ^{1}H NMR ($CDCl_3$) δ 0.90 (m, 6H), 1.56 (q, 2H), 1.67 (q, 2H), 2.53 (t, 2H), 3.43 (m, 2H), 3.59 (m, 4H), 3.93 (m, 4H) ppm. Anal. ($C_{11}H_{22}LiO_6PS$) C, H.

Lithium methyl (2*R*)-3-(propyloxy)-2-(octanoylthio)-1-propyl phosphate (22b): ^{1}H NMR ($CDCl_3$) δ 0.90 (m, 6H), 1.29 (m, 8H), 1.60 (m, 4H), 2.55 (t, 2H), 3.45 (m, 3H), 3.60 (d, 3H), 3.65 (m, 1H, 4.00 (br m, 3H). Anal. ($C_{15}H_{30}LiO_6PS$) C, H.

Lithium methyl (2*R*)-3-(pentyloxy)-2-(butanoylthio)-1-propyl phosphate (22c): ^{1}H NMR ($CDCl_3$) δ 0.90 (m, 6H), 1.29 (m, 4H), 1.53 (m, 2H), 1.66 (q, 2H), 2.53 (t, 2H), 3.45 (m, 2H), 3.60 (m, 5H), 3.96 (m, 3H) ppm. Anal. ($C_{13}H_{26}LiO_6PS$) C, H.

Lithium methyl (2*R*)-3-(pentyloxy)-2-(octanoylthio)-1-propyl phosphate (22d): ^{1}H NMR ($CDCl_3$) δ 0.85 (m, 6H), 1.23 (m, 12H), 1.60 (m, 4H), 2.52 (t, 2H), 3.44 (m, 2H), 3.56 (d, 3H), 3.63 (m, 2H), 3.87 (m, 2H), 4.02 (m, 1H) ppm. Anal. ($C_{17}H_{34}LiO_6PS$) C, H.

Lithium methyl (2*R*)-3-(octyloxy)-2-(butanoylthio)-1-propyl phosphate (22e): ^{1}H NMR ($CDCl_3$) δ 0.91 (m, 6H), 1.28 (m, 10H), 1.55 (m, 2H), 1.67 (q, 2H), 2.53 (t, 2H), 3.45 (m, 4H), 3.60 (m, 3H), 3.97 (m, 3H) ppm. Anal. Calcd for $C_{16}H_{32}LiO_6PS$: C, 49.21; H, 8.27. Found: C, 49.95; H, 8.17.

Lithium methyl (2*R*)-3-(octyloxy)-2-(octanoylthio)-1-propyl phosphate (22f): ^{1}H NMR ($CDCl_3$) δ 0.87 (m, 6H), 1.27 (br s, 21H), 1.57 (m, 4H), 2.53 (t, 2H), 3.44 (m, 2H), 3.57 (d, 3H), 3.65 (br s, 2H), 3.96 (m, 3H) ppm. Anal. Calcd for $C_{20}H_{40}LiO_6PS$: C, 53.78; H, 9.04. Found: C, 54.55; H, 8.93.

General Procedure: Detritylation, Phosphorylation, and Dealkylation of 19g–p. Conversion of trityl ethers **19g–p** to lithium phosphates **22g–p** was conducted according to the related procedures in Scheme 2.

Lithium (2*R*)-3-(benzyloxy)-2-(decanoylthio)-1-propyl methyl phosphate (22g): ^{1}H NMR (DMSO-d_6) δ 0.84 (t, 3H), 1.23 (br s, 7H), 1.52 (m, 2H), 2.48 (s, 3H), 2.54 (t, 2H), 3.26 (d, 3H), 3.31 (br s, 2H), 3.56 (m, 2H), 3.92 (m, 3H), 4.48 (AB q, 2H), 7.30 (m, 5H) ppm. Anal. ($C_{21}H_{34}LiO_6PS$) C, H, S.

Lithium methyl (2*R*)-3-[(4-phenylbenzyl)oxy]-2-(decanoylthio)-1-propyl phosphate (22h): ^{1}H NMR (DMSO-d_6) δ 0.82 (t, 3H), 1.10–1.33 (m, 12H), 1.48–1.60 (m, 2H), 2,55 (t, 2H), 3.27 (d, 3H), 3.56–3.83 (m, 5H), 4.53 (s, 2H), 7.28–7.70 (m, 9H) ppm. Anal. ($C_{27}H_{38}LiO_6PS{\cdot}0.5H_2O$) C, H, S.

Lithium methyl (2*R*)-3-[(4-phenoxybenzyl)oxy]-2-(decanoylthio)-1-propyl phosphate (22i): ^{1}H NMR (DMSO-d_6) δ 0.92 (t, 3H), 1.05–1.31 (m, 12H), 2.52 (t, 2H), 3.25 (d, 3H), 3.59 (m, 2H), 3.79 (m, 3H), 4.44 (s, 2H), 6.91–7.45 (m, 9H) ppm. Anal. ($C_{27}H_{38}LiO_7PS$) C, H.

Lithium methyl (2*R*)-3-[[(2*E*)-3-phenyl-2-propen-1-yl]oxy]-2-(decanoylthio)-1-propyl phosphate (22j): ^{1}H NMR (DMSO-d_6) δ 0.82 (t, 3H), 1.05–1.35 (m, 12H), 1.40–1.63 (m, 2H), 2.55 (t, 2H), 3.27 (d, 3H), 3.50–3.82 (m, 5H), 4.05–4.15 (m, 2H), 6.24–6.64 (m, 2H), 7.15–7.50 (m, 5H) ppm. Anal. ($C_{23}H_{36}LiO_6PS$) C, H, S.

Lithium (2*R*)-3-(3,3-dimethylbutoxy)-2-(decanoylthio)-1-propyl methyl phosphate (22k): ^{1}H NMR (DMSO-d_6) δ 0.80–0.90 (m, 12H), 1.17–1.30 (m, 12H), 1.40 (t, 2H), 1.46–1.60 (m, 2H), 2.55 (t, 2H), 3.27 (d, 3H), 3.41 (t, 2H), 3.45–3.52 (m, 2H), 3.62–3.73 (m, 3H) ppm. Anal. ($C_{20}H_{40}LiO_6PS$) C, H, S.

Lithium methyl (2*R*)-3-[(2*Z*)-2-penten-1-yloxy]-2-(decanoylthio)-1-propyl phosphate (22l): ^{1}H NMR (DMSO-d_6) δ 0.78–0.88 (m, 6H), 1.15–1.40 (m, 14H), 1.46–1.60 (m, 2H), 1.90–2.04 (m, 2H), 2.55 (t, 2H), 3.27 (d, 3H), 3.42–3.53 (m, 2H), 3.63–3.77 (m, 3H), 3.87 (d, 2H), 5.38–5.70 (m, 2H) ppm. Anal. ($C_{20}H_{38}LiO_6PS$) C, H, S.

Lithium (2*R*)-3-(hexyloxy)-2-[(4-methylpentanoyl)thio]-1-propyl methyl phosphate (22m): ^{1}H NMR (DMSO-d_6) δ 0.78–0.88 (m, 9H), 1.18–1.33 (m, 6H), 1.38–1.59 (m, 5H), 2.55 (t, 2H), 3.27 (d, 3H), 3.36 (t, 2H), 3.44–3.52 (m, 2H), 3.62–3.74 (m, 3H) ppm. Anal. ($C_{16}H_{32}LiO_6PS$) C, H, S.

Lithium methyl (2*R*)-3-(hexyloxy)-2-[(3-phenylpropanoyl)thio]-1-propyl phosphate (22n): ^{1}H NMR (DMSO-d_6) δ 0.85 (t, 3H), 1.18–1.32 (m, 6H), 1.38–1.50 (m, 2H), 2.87 (s, 4H), 3.24–3.38 (m, 5H), 3.42–3.49 (m, 2H), 3.63–3.75 (m, 3H), 7.10–7.30 (m, 5H) ppm. Anal. ($C_{19}H_{30}LiO_6PS$) C, H, S.

Lithium (2*R*)-3-(hexyloxy)-2-[(2*E*)-2-pentenoylthio]-1-propyl methyl phosphate (22o): ^{1}H NMR (DMSO-d_6) δ 0.78–0.96 (m, 6H), 1.18–1.33 (m, 6H), 1.38–1.53 (m, 2H), 1.92–2.05 (m, 2H), 3.20–3.40 (m, 7H), 3.42–3.53 (m, 2H), 3.62–3.78 (m, 3H), 5.35–5.72 (m, 2H) ppm. Anal. ($C_{16}H_{30}LiO_6PS$) C, H, S.

Lithium (2*R*)-3-(hexyloxy)-2-(benzoylthio)-1-propyl methyl phosphate (22p). The above protected alcohol was deprotected and phosphorylated using procedures previously described (Scheme 2) to afford compound **22p** as a white solid: ^{1}H NMR (DMSO-d_6) δ 0.82 (t, 3H), 1.15–1.35 (m, 6H), 1.40–1.53 (m, 2H), 3.26–3.45 (m, 5H), 3.55–3.65 (m, 2H), 3.73–3.90 (m, 3H), 7.50–7.95 (m, 5H) ppm. Anal. ($C_{17}H_{26}LiO_6PS$) C, H, S.

Acknowledgment. The authors gratefully acknowledge G. Chandra, I. Patel, and T. Kost for cloning and expression of the hs-PLA$_2$, L. Overton and C. Barrett for cells expressing the recombinant protein, and M. Luther, B. Ellis, and P. DeLacy for protein purification. We thank P. Brown, D. Karanewsky, and J. S. Wiseman for helpful discussions.

References

(1) Glaser, K. B.; Mobilio, D.; Chang, J. Y.; Senko, N. Phospholipase A$_2$ Enzymes: Regulation and Inhibition. *Trends Pharmacol. Sci.* **1993**, *14*, 90–98. (b) Mobilio, D.; Marshall, L. A. Recent Advances in the Design and Evaluation of Inhibitors of PLA$_2$. *Annu. Rep. Med. Chem.* **1989**, *24*, 157–166. (c) Dennis, E. A. Regulation of Eicosanoid Production: Role of Phospholipases and Inhibitors. *Bio/Technology* **1987**, *5*, 1294–1300.

(2) (a) Pruzanski, W.; Vadas, P.; Stefanski, E.; Urowitz, M. B. Phospholipase A$_2$ Activity in Sera and Synovial Fluids in Rheumatoid Arthritis and Osteoarthritis. Its Possible Role as a Proinflammatory Enzyme. *J. Rheumatol.* **1988**, *12*, 211–216. (b) Hara, S.; Kudo, I.; Chang, H. W.; Matsuta, K.; Miyamato, T.; Inoue, K. Purification and Characterization of Extracellular Phospholipase A$_2$ from Human Synovial Fluid in Rheumatoid Arthritis. *J. Biochem.* **1989**, *105*, 395–399. (c) Vadas, P.; Pruzanski, W.; Stefanski, E.; Sternby, B. Compartmental Heterogeneity of Soluble Phospholipases A$_2$. *Inflammation* **1990**, *14*, 173–183.

(3) (a) Vadas, P.; Pruzanski, W.; Stefanski, E.; Ruse, J.; Farewell, V.; McLaughlin, J.; Bombardier, C. Concordance of Endogenous Cortisol and Phospholipase A$_2$ Levels in Gram-Negative Septic Shock: A Prospective Study. *J. Lab. Clin. Med.* **1988**, *111*, 584. (b) Aufenanger, J.; Zimmer, W.; Kattermann, R. Characteristics and Clinical Application of a Radiometric Escherichia Coli-Based Phospholipase A$_2$ Assay Modified for Serum Analysis. *Clin. Chem.* **1993**, *39*, 605–613.

(4) (a) Vadas, P.; Pruzanski, W.; Kim, J.; Fornasier, V. The Proinflammatory Effect of Inter-Articular Injection of Soluble Human and Venom Phospholipase A$_2$. *Am. J. Pathol.* **1989**, *134*, 807–811. (b) Bomalaski, J. S.; Lawton, P.; Browning, J. L. Human Extracellular Recombinant Phospholipase A$_2$ Induces an Inflammatory Response in Rabbits. *J. Immunol.* **1991**, *146*, 3904–3910.

(5) (a) Jain, M. K.; Ghomashchi, F.; Yu, B. Z.; Bayburt, T.; Murphy, D.; Houck, D.; Brownell, J.; Reid, J. C.; Solowilj, J. E. Fatty Acid Amides: Scooting Mode-Based Discovery of Tight-Binding Competitive Inhibitors of Secreted Phospholipases A$_2$. *J. Med. Chem.* **1992**, *35*, 3584–6. (b) Bayburt, T.; Yu, B. Z.; Lin, H. K.; Browning, J.; Jain, M. K.; Gelb, M. H. Human Nonpancreatic Secreted Phospholipases A$_2$: Interfacial Parameters, Substrate Specificities, and Competitive Inhibitors. *Biochemistry* **1993**, *32*, 573–82. (c) van Oort, M. G.; Dijkman, R.; Hille, J. D. R.; de Haas, G. H. Kinetic Behavior of Porcine Pancreatic Phospholipase A$_2$ on Zwitterionic and Negatively Charged Single-Chain Substrates. *Biochemistry* **1985**, *24*, 7987–93. (d) Yuan, W.; Quinn, D. M.; Sigler, P. B.; Gelb, M. H. Kinetic and inhibition Studies of Phospholipase A$_2$ with Short-Chain Substrates and Inhibitors. *Biochemistry* **1990**, *29*, 6082–94.

(6) Dijkstra, B. W.; Kalk, K. H.; Hol, W. G. J.; Drenth, J. Structure of Bovine Pancreatic Phospholipase A$_2$ at 1.7 Å Resolution. *J. Mol. Biol.* **1981**, *147*, 97–123.

(7) Brunie, S.; Bolin, J.; Gewirth, D.; Sigler, P. B. The Refined Crystal Structure of Dimeric Phospholipase A$_2$ at 2.5 Å. *J. Biol. Chem.* **1985**, *260*, 9742–9749.

(8) Wery, J.-P.; Schevitz, R. W.; Clawson, D. K.; Bobbitt, J. L.; Dow, E. R.; Gamboa, G.; Goodson, Jr., T.; Hermann, R. B.; Kramer. R. M.; McClure, D. B.; Mihelich, E. D.; Putnam, J. E.; Sharp, J. D.; Stark; D. H.; Warrick, M. W.; Jones, N. D. Structure of Recombinant Human Rheumatoid Arthritic Synovial Fluid Phospholipase A_2 at 2.2 Å Resolution. *Nature* **1991**, *352*, 79–82.

(9) Scott, D. L.; White, S. P.; Browning, J. L.; Rosa, J. J.; Gelb, M. H.; Sigler, P. B. Structures of Free and Inhibited Human Secretory Phospholipase A_2 from Inflammatory Exudate. *Science* **1991**, *254*, 1007–1010.

(10) Thunnissen, M. G. M.; Ab, E.; Kalk, K. H.; Drenth, J.; Dijkstra, B. W.; Kuipers, O. P.; Dijkman, R.; de Haas, G. H.; Verheij, H. M. X-Ray Structure of Phospholipase A_2 Complexed With a Substrate-Derived Inhibitor. *Nature* **1990**, *347*, 689–691.

(11) White, S. P.; Scott, D. L.; Otwinowski, Z.; Gelb, M. H.; Sigler, P. B. Crystal Structure of Cobra-Venom Phospholipase A_2 in a Complex with a Transition-State Analogue. *Science* **1990**, *250*, 1560–1563.

(12) The pH of the reaction was maintained at 9 by titration with 1 mM NaOH using a pH-stat (Radiometer Copenhagen VIT90 with ABU91 autoburette). The putative substrates (100 μM) were dissolved in deionized water containing 2 mM Ca^{2+}. The reaction vessel was washed with a gentle stream of nitrogen to minimize background drift due to absorption of atmospheric CO_2. hs-PLA_2 (1.69 nmol, 2.41 μg) was added to start the reaction, and the rate of hydrolysis was recorded for 1 h. Rates of hydrolysis were calculated from the observed rate of base consumption.

(13) Recombinant hs-PLA_2 used in these studies was purified from a baculovirus expression system by a series of standard chromatographic steps; final purification was by reversed-phase HPLC. Details of the enzyme preparation will be given elsewhere. Preliminary studies (Table 1 *only*) were obtained using enzyme expressed in *E. coli*.

(14) Turnover of the thioester analogs was measured spectrophotometrically using 5,5′-dithiobis(2-nitrobenzoic) acid (DTNB) to detect the free thiol groups generated. Hydrolysis rates (nmol/min) were calculated from the observed rate of absorbance change at 405 nm using an extinction coefficient for the thionitrobenzoate anion of 13 600 M^{-1}. The apparent k_{cat}/K_m's were calculated based on the slope of a (linear) plot of rate *versus* substrate concentration and the known concentration of enzyme as outlined below. The buffer used was 20 mM HEPES, pH 7.5, containing 2 mM Ca^{2+} and 0.8 mM DTNB. The enzyme concentration was 14 nM.

(15) cLogP values were calculated with the CLOGP program, version 3.55, from Daylight Chemical Information Systems, Inc., Irvine, CA. log *P* values are generally difficult to interpret for charged molecules. Consequently, for this work, the charged *sn*-3 phosphate head group was replaced by an *sn*-3 hydroxyl group for the calculation of the cLogP.

(16) DeVendittis, E.; Palumbo, G.; Palato, G.; Bocchini, V. A Fluorometric Method for the Estimation of the Critical Micelle Concentration of Surfactants. *Anal. Biochem.* **1981**, *115*, 278–286.

(17) Martin, S. F.; Josey, J. A. A General Protocol for the Preparation of Phospholipids via Phosphite Coupling. *Tetrahedron Lett.* **1988**, *29*, 3631–4.

(18) *(a)* Kim, U. T.; Bhatia, S. K.; Hajdu, J. Stereospecific Synthesis of Ether Phospholipids. Preparation of 1-O-octadecyl-2-alkylaminodeoxyglycerophosphocholines. *Tetrahedron Lett.* **1991**, *32*, 6521–6524. (b) Baker, S. R.; Harris, J. R. A Convenient Synthesis of Some 1,4-Disubstituted 7-oxabicyclo [2.2.1]heptanes. *Synth. Commun.* **1991**, *21*, 2015–2023.

(19) Aarsman, A. J.; Rosenboom, C. F. P.; VanderMarel, G. A.; Shadid, B.; VanBoom, J. H.; VandenBosch, H. Synthesis of Acylthioester Phospholipids and Their Hydrolysis by Phospholipase A_2. *Chem. Phys. Lipids* **1985**, *36*, 229–242.

(20) Insight II versions 1.0 and 1.1, Homology version 1.0, Discover versions 2.5 and 2.6, from Biosym Technologies, 9685 Scranton Rd, San Diego, CA.

(21) (a) Gibson, K. D.; Scheraga, H. A. Revised Algorithms for the Build-Up Procedure for Predicting Protein Conformations by Energy Minimization. *J. Computat. Chem.* **1987**, *8*, 826–834. (b) Milburn, M. V.; Hassell, A. M.; Lambert, M. H.; Jordan, S. R.; Proudfoot, A. E. I.; Graber, P.; Wells, T. N. C. A novel dimer configuration revealed by the crystal structure at 2.4 Å resolution of human interleukin-5. *Nature* **1993**, *363*, 172–176.

(22) Dauber-Osguthorpe, P.; Roberts, V. A.; Osguthorpe, D. J.; Wolff, J.; Genest, M.; Hagler, A. T. Structure and Energetics of Ligand Binding to Proteins: Escherichia coli Dihydrofolate Reductase-Trimethoprim, A Drug-Receptor System. *Proteins* 1988, *4*, 31–47.

(23) Stewart, J. J. P. Optimization of Parameters for Semiempirical Methods I. Method. *J. Comput Chem.* **1989**, *10*, 209–220.

(24) Allen, F. H.; Bellard, S.; Brice, M. D.; Cartwright, B. A.; Doubleday, A.; Higgs, H.; Hummelink, T.; Hummelink-Peters, B. G.; Kennard, O.; Motherwell, W. D. S.; Rodgers, J. R.; Watson, D. G. The Cambridge Crystallographic Data Centre: Computer-Based Search, Retrieval, Analysis and Display of Information. *Acta Crystallogr.* **1979**, *B35*, 2331–2339.

(25) Spartan version 2.0, from Wavefunction, Inc., 18401 Von Karman Ave, Irvine, CA.

(26) Beaton, H. G.; Bennion, C.; Connolly, S.; Cook, A. R.; Gensmantel, N. P.; Hallam, C.; Hardy, K.; Hitchin, B.; Jackson, C. G.; Robinson, D. H. Discovery of New Non-Phospholipid Inhibitors of the Secretory Phospholipases A_2. *J. Med. Chem.* **1994**, *37*, 557–9.